Appl Microbiol Biotechnol
DOI 10.1007/s00253-014-5807-3

Quorum quenching is an antivirulence strategy employed by endophytic bacteria

Parijat Kusari · Souvik Kusari · Marc Lamshöft · Selahaddin Sezgin · Michael Spiteller · Oliver Kayser

Received: 17 February 2014 / Revised: 22 April 2014 / Accepted: 26 April 2014

Abstract Bacteria predominantly use quorum sensing to regulate a plethora of physiological activities such as cell-cell crosstalk, mutualism, virulence, competence, biofilm formation, and antibiotic resistance. In this study, we investigated how certain potent endophytic bacteria harbored in *Cannabis sativa* L. plants use quorum quenching as an antivirulence strategy to disrupt the cell-to-cell quorum sensing signals in the biosensor strain, *Chromobacterium violaceum*. We used a combination of high-performance liquid chromatography high-resolution mass spectrometry (HPLC-ESI-HRMS^n) and matrix-assisted laser desorption ionization imaging high-resolution mass spectrometry (MALDI-imaging-HRMS) to first quantify and visualize the spatial distribution of the quorum sensing molecules in the biosensor strain, *C. violaceum*. We then showed, both quantitatively and visually in high spatial resolution, how selected endophytic bacteria of *C. sativa* can selectively and differentially quench the quorum sensing molecules of *C. violaceum*. This study provides fundamental insights into the antivirulence strategies used by endophytes in order to survive in their ecological niches. Such defense mechanisms are evolved in order to thwart the plethora of pathogens invading associated host plants in a manner that prevents the pathogens from developing resistance against the plant/endophyte bioactive secondary metabolites. This work also provides evidence towards utilizing endophytes as tools for biological control of bacterial phytopathogens. In continuation, such insights would even afford new concepts and strategies in the future for combating drug resistant bacteria by quorum-inhibiting clinical therapies.

Keywords Bacterial endophytes · Quorum quenching · *N*-acylated homoserine lactones · *Cannabis sativa* L · High-resolution mass spectrometry · MALDI imaging high-resolution mass spectrometry · Microbe-microbe interaction · Microbe-plant interaction · Phytopathology

Introduction

Quorum sensing is one of the intrinsic chemical cell-to-cell signaling cascades in bacteria that facilitate invasion, colonization of particular niches, and pathogenesis of a plethora of organisms, ranging from unicellular prokaryotes to multicellular eukaryotes (Hosni et al. 2011). *N*-acylated L-homoserine lactones (AHLs) of Gram-negative bacteria and oligopeptides of Gram-positive bacteria are released as autoinducers to facilitate quorum sensing (LaSarre and Federle 2013). These in turn coordinate responses across a population to establish crosstalk, the most important being able to thwart chemical defenses (e.g., production of antibiotic compounds) of other organisms (Teplitski et al. 2011). Over the last decades, quorum sensing has progressively received attention in clinical studies owing to an increasing drug resistance in pathogenic bacteria that is a dreaded challenge in curing current and emerging life-threatening diseases. Therefore, alternate "antivirulence" strategies are being sought to target quorum sensing in pathogenic bacteria (Amara et al. 2011; Burmølle et al. 2010; Claessen et al. 2014). Inhibition of quorum sensing in pathogenic bacteria, a process known as "quorum quenching", has a fundamental advantage over other disease-management strategies (such as antimicrobial

Souvik Kusari and Marc Lamshöft contributed equally to this work.

P. Kusari · O. Kayser (✉)
Department of Biochemical and Chemical Engineering, TU Dortmund, Emil-Figge-Str. 66, 44227 Dortmund, Germany
e-mail: Oliver.Kayser@bci.tu-dortmund.de

S. Kusari · M. Lamshöft · S. Sezgin · M. Spiteller (✉)
Institute of Environmental Research (INFU), Department of Chemistry and Chemical Biology, TU Dortmund, Otto-Hahn-Str. 6, 44221 Dortmund, Germany
e-mail: spiteller@infu.tu-dortmund.de

Published online: 21 May 2014

therapies) and opens new approaches to tackle drug-resistant bacteria. Targeting quorum sensing in a pathogenic bacterial population mitigates virulence as opposed to suppressing bacterial growth and therefore, does not introduce any selective pressure for developing drug (or antibiotic) resistance (Clatworthy et al. 2007; Rasko and Sperandio 2010; LaSarre and Federle 2013).

Beyond the clinical setting, quorum sensing is also crucially relevant in microbe-microbe and plant-microbe crosstalk in almost all ecological niches (Safari et al. 2014). In the recent years, a promising group of microorganisms called "endophytes" have garnered attention owing to their potential utility in the pharmaceutical and agricultural sectors (Porras-Alfaro and Bayman 2011; Kusari and Spiteller 2011; Kharwar et al. 2011; Aly et al. 2013; Kusari et al. 2014). These diverse groups of microorganisms inhabit the internal tissues of plant without any manifestation of disease for a part of their life cycle and engage in multipartite interactions with other organisms (host plant, associated endophytes, invading pathogens, pests, and feeders). Such interactions lead to the development of different functional traits in endophytes such as synthesizing bioactive secondary metabolites, controlling plant diseases by quorum quenching, and even aiding in plant tolerance towards environmental stress like drought and salinity (Kusari et al. 2012, 2013, 2014).

In this study, we quantified and visualized the distribution and modulation of cell-to-cell signaling communication system of the biosensor strain, *Chromobacterium violaceum*, and further quenching of the quorum coordination by potent endophytic bacteria harbored in *Cannabis sativa* L. plants. *C. sativa* is a medicinal plant that contains pharmaceutically relevant cannabinoids such as delta 9-tetrahydrocannabinol (Taura et al. 2007; Grotenhermen and Müller-Vahl 2012). Our earlier investigation of the endophytic fungal community of this plant with regard to their attack-defense ecological strategies against host plant-specific phytopathogens revealed their potential as biocontrol agents (Kusari et al. 2013). This further prompted us to investigate the endophytic bacterial community harbored in the same plant and their ecological roles in host-plant fitness. Using high-performance liquid chromatography coupled to high-resolution mass spectrometry with electrospray ionization (HPLC-ESI-HRMS^n), we have proved that potent endophytic bacteria target and quench four different AHLs [*N*-hexanoyl-L-homoserine lactone (C6-HSL), *N*-octanoyl-L-homoserine lactone (C8-HSL), *N*-decanoyl-L-homoserine lactone (C10-HSL), and *N*-(3-oxo-decanoyl)-L-homoserine lactone (3-oxo-C10-HSL)] used by *C. violaceum* for violacein-mediated quorum sensing. We further used matrix-assisted laser desorption ionization imaging high-resolution mass spectrometry (MALDI-imaging-HRMS) to show the spatial localization of each AHL by *C. violaceum* and the concomitant selective impediment of the AHLs by bacterial endophytes. MALDI-imaging mass spectrometry has gained impetus in natural products research for elucidating organismal interactions by visualizing the exact location of biosynthesis and distribution of target and nontarget compounds in vitro and in vivo (Rompp and Spengler 2013; Shih et al. 2014; Bjarnholt et al. 2014). To the best of our knowledge, this is the first report of "visualizing" quorum sensing and quorum quenching using MALDI-imaging high-resolution mass spectrometry.

Materials and methods

Collection and authentication of plant material

C. sativa L. plants were sampled from the Bedrocan BV Medicinal Cannabis (Veendam, Netherlands). The plants were identified and authenticated as *C. sativa* L. by experienced botanists at the Bedrocan BV. Plants specimens are under deposit at Bedrocan BV with voucher numbers (A1)05.41.050710. Import of the plant material was allowed according to the permission of the Federal Institute for Drugs and Medical Devices (Bundesinstituts für Arzneimittel und Medizinprodukte, BfArM), Bonn, Germany under the license number 458 49 89. The plant material was transported to TU Dortmund, Germany in sealed plastic ziplock bags at 4 °C and processed for the isolation of endophytes within 6 h of plant collection.

Isolation and establishment of in vitro axenic cultures of endophytic bacteria

The plant materials were excised in small fragments (~20 mm length) with the aid of flame-sterilized razor blade. The excised explants were washed thoroughly under running tap water followed by deionized water (DI) to remove any dirt attached to them. The explants were then surface sterilized following previously established procedures (Kusari et al. 2009a). Briefly, the small fragments were surface sterilized by sequential immersion in 70 % ethanol for 1 min, 1.3 M sodium hypochlorite (3–5 % available chlorine) for 3 min, and 70 % ethanol for 30 s. Finally, these surface-sterilized tissue pieces were rinsed thoroughly in sterile, double-distilled water for a couple of minutes, to remove excess surface sterilants. The excess moisture was blotted on sterile filter paper. The surface-sterilized tissue fragments were placed in sterile mortar-pestle and crushed with the addition of sterile double-distilled water. The macerated tissues, thus obtained, were carefully plated on Petri dishes containing nutrient agar (NA). The Petri dishes were sealed using parafilm and incubated at 28±2 °C. To ensure proper surface sterilization, three different techniques were implemented. Firstly, the sterile double-distilled water of the final rinse were plated on NA and incubated in parallel under similar conditions. Secondly,

the surface-sterilized tissue fragments were imprinted simultaneously in NA and incubated under similar conditions (secondary protocol, "imprint technique") (Schulz et al. 1998; Sánchez Márquez et al. 2007). Finally, the unsterilized fragments (only washed in tap water followed by deionized water) were prepared simultaneously and incubated in parallel to isolate the surface-contaminating bacterial isolates and further differentiated by both macroscopic and microscopic evaluation (Kusari et al. 2009b). The cultures were monitored every day to check the growth of bacterial colonies. The bacterial colonies which grew on the plates after few days were subcultured successively onto fresh NA plates and incubated at 28±2 °C, and finally isolated as axenic strains. The endophytic bacterial isolates were routinely maintained on NA plates in active form and preserved in 15 % (*v*/*v*) glycerol at −80 °C for long-term storage. The endophytic bacterial isolates were assigned suitable strain designations (see Table 1) and were deposited in the internal culture collection of Technical Biochemistry, TU Dortmund, Germany.

Genomic DNA extraction, amplification of 16S rRNA gene, and sequencing

A set of 500 mL capacity conical flasks, each with 100 mL autoclaved nutrient broth (NB; Roth, Karlsruhe, Germany), were used for the isolation of genomic DNA of bacterial endophytes. A loop full of each bacterial isolate from the parent axenic culture was inoculated in the respective flasks containing NB and incubated at 28±2 °C with proper shaking (150 rev min^{-1}) on a rotary shaker (INFORS HT Multitron 2, Einsbach, Germany) for 24–36 h depending on the growth kinetics of each endophytic bacterium. The growth kinetics was monitored by measuring the optical density at 600 nm (OD_{600}). The bacterial isolates were grown until the mid-log phase ("steady state") for extraction of genomic DNA. The total genomic DNA was extracted using peqGOLD bacterial DNA kit (Peqlab Biotechnologie GmbH, Erlangen, Germany) strictly following the manufacturer's guidelines. The DNA was then subjected to PCR amplification using the primers 27f and 1492r (Lane 1991).

The PCR amplification was performed in a 50 μL reaction mixture containing 10 μL Phusion HF buffer (5×), 1 μL dNTPs (10 mM), 0.5 μL forward primer (100 μM), 0.5 μL reverse primer (100 μM), 3 μL of template DNA, 1 μL of Phusion polymerase (2U μL^{-1}; Fermentas, Thermo Scientific, Schwerte, Germany), and 34 μL of sterile double-distilled water. The PCR cycling conditions consisted of an initial denaturation at 98 °C for 3 min, 30 cycles of denaturation, annealing, and elongation at 98 °C for 10 s, 60 °C for 30 s, and 72 °C for 45 s. This was followed by a final elongation step of 72 °C for 10 min. As a negative control, the template DNA was replaced by sterile double-distilled water. The PCR-amplified products obtained were approximately around 1,500 base pairs (bp) and were visualized by gel electrophoresis. The products were further purified using peqGOLD MicroSpin Cycle Pure Kit (Peqlab Biotechnologie GmbH, Erlangen, Germany) strictly following manufacturer's instructions. The amplified products were then sequenced from both directions at GATC Biotech (Cologne, Germany) using the above-mentioned primers.

The sequences of all the endophytic bacteria under this study have been deposited at the EMBL-Bank under the accession numbers HG424705 to HG42717 (see Table 1).

Preparation of cell-free supernatant

The cell-free supernatant (CFS) was prepared according to previously established methods, suitably modified (Rishi et al.

Table 1 16S rRNA-based identification of bacterial endophytes isolated from *Cannabis sativa* L. plants with their respective strain codes and the EMBL-Bank accession numbers

Strain number (endophyte)	EMBL-Bank accession number	Most closely related species (accession number)	Maximum identity (%)
B1	HG424705	*Bacillus licheniformis* (AB055006.1)	99
B2	HG424706	*Bacillus licheniformis* (KF040981.1)	99
B3	HG424707	*Bacillus* sp. (JQ808527.1)	99
B4	HG424708	*Bacillus megaterium* (KC443085.1)	99
B5	HG424709	*Bacillus pumilus* (EU500930.1)	99
B6	HG424710	*Bacillus licheniformis* (KF148636.1)	97
B7	HG424711	*Bacillus pumilus* (JQ798393.1)	98
B8	HG424712	*Brevibacillus borstelensis* (JQ229800.1)	98
B9	HG424713	*Bacillus* sp. (JQ678041.1)	99
B10	HG424714	*Bacillus subtilis* (JX123316.1)	99
B11	HG424715	*Bacillus* sp. (FJ908092.1)	99
B12	HG424716	*Mycobacterium peregrinum* (JX266704.1)	99
B13	HG424717	*Mycobacterium* sp. (HE575961.1)	99

2011; Ou et al. 2009; Zhao et al. 2011). A set of conical flasks of 300 mL capacity, each with 50 mL autoclaved NB, was used. Each bacterial isolate was inoculated in respective flasks from their parent axenic cultures and incubated at 28±2 °C with proper shaking (150 rev min^{-1}) on a rotary shaker (INFORS HT Multitron 2, Einsbach, Germany) until the mid-log phase. The bacterial cultures were centrifuged at 10,000 rpm for 30 min at 4 °C. For the preparation of CFS, the supernatant was separated from the cell pellets and filtered twice through sterile 0.22 μm Rotilabo®-Spritzenfilter (Carl Roth GmbH) for the complete removal of cells. The CFS of each endophytic bacterial isolate was serially diluted to a factor of 10^{-4} to 10^{-8}, and 100 μL were spread on NA plates to check for any bacterial contamination.

Quorum-sensing/quenching activity of the endophytic isolates

The type strain *C. violaceum* (accession number DSM 30191) was obtained from Leibniz Institute DSMZ-German Collection of Microorganisms and Cell Cultures, Braunschweig, Germany. The activation of the bacterial strain was performed according to DSMZ guidelines. The medium used for the activation was NB (Roth). *C. violaceum* was routinely maintained on NA and cultured aerobically in NB at 30 °C with proper shaking (150 rev min^{-1}). To determine the quorum sensing and/or quenching responses of the endophytic bacterial isolates, spectrophotometric quantitation of violacein was analyzed according to previously established procedure, suitably modified (Limsuwan and Voravuthikunchai 2008; Thenmozhi et al. 2009). *C. violaceum* was grown overnight in NB until OD_{600} of 0.1 was achieved. A set of conical flasks of 300 mL capacity, each with 10 mL NB seeded with 1 mL overnight culture (OD_{600} of 0.1) of *C. violaceum*, was used. The conical flasks contained 1, 2, 4, and 8 mL of CFS, respectively. As a control, equal volumes of NB were added to the respective control flasks. All the flasks were incubated overnight at 30 °C with proper shaking (150 rev min^{-1}). One milliliter of culture from each of the flasks was centrifuged at 13,000 rpm for 10 min for precipitation of insoluble violacein. One milliliter dimethyl sulfoxide (DMSO) was added to the cell pellets and vortexed vigorously for 1 min to solubilize the violacein completely. The solution was centrifuged again at 13,000 rpm for 5 min to remove the cell debris. The supernatant was then quantified spectrophotometrically at OD_{585}. Each setup was prepared in triplicates (biological replicates) and the quantitation was repeated thrice (technical replicates). One milliliter culture from each of the setups was serially diluted to a factor of 10^{-4} to 10^{-8}, and 100 μL was spread on NA plates to check for any bacterial contamination.

Furthermore, a suitably modified colony forming units (CFU/mL) assay (Choo et al. 2006) was also performed to confirm that the CFS extracts significantly reduced only the violacein production but did not have any effect on the growth of *C. violaceum*. Briefly, 1 mL culture from each of the experimental setups (CFS treated) and control (untreated) was serially diluted from 10^{-4} to 10^{-8}. 10 μL (at dilution of 10^{-8}) was spread on NA plates and incubated overnight at 30 °C. Each cell count was repeated twice.

Sample preparation for analytical measurements

The endophytic isolates showing quorum quenching responses in the flask assay were further analyzed via high-performance liquid chromatography high-resolution mass spectrometry ($LC\text{-}FTMS^n$). A set of conical flasks of 500 mL capacity, each with 200 mL NB and 1 mL overnight culture (OD_{600} of 0.1) of *C. violaceum*, was used. CFS of the isolates showing quorum quenching responses was added to the respective flasks. NB was used as a control. The flasks were incubated overnight at 30 °C with proper shaking (150 rev min^{-1}). The cultures were centrifuged at 13,000 rpm for 30 min. Ten microliters of internal standard d_3-C6-HSL (0.1 mg mL^{-1}) was added to the spent supernatant and extracted twice with an equal volume of ethyl acetate. The organic extracts were evaporated to vacuum and reconstituted in 1 mL HPLC-grade methanol. The methanolic extracts were subjected to mass spectrometry. The *C. violaceum* culture alone (with NB instead of CFS) was extracted as a positive control. The NB alone was extracted as a negative control. The mass spectrometric analysis was performed in duplicates.

Preparation of standards

All standard compounds C6-HSL, C8-HSL, 3-oxo-C10-HSL, and C10-HSL and the internal standard d_3-C6-HSL were purchased from Sigma-Aldrich, Steinheim, Germany and were dissolved in HPLC-grade methanol at a concentration of 0.1 mg mL^{-1}. Calibration standards (2, 5, 20, 50, 200, 500, 2,000, and 5,000 ng mL^{-1}) were prepared by serial dilution of the stock solutions containing in addition, an absolute 100 ng of the internal standard in methanol/water (1:4).

High-resolution mass spectrometry

The high-resolution mass spectra were obtained with an LTQ-Orbitrap Spectrometer (Thermo Fisher, MA, USA) equipped with a HESI-II source. The spectrometer was operated in positive mode (1 spectrum s^{-1}; mass range, 180–600) with nominal mass resolving power of 60,000 at *m/z* 400 with a scan rate of 1 Hz) with automatic gain control to provide high-accuracy mass measurements within 2 ppm deviation using an internal standard; *bis*(2-ethylhexyl)phthalate, *m/z*= 391.284286. The spectrometer was attached with an Agilent (Santa Clara, USA) 1200 HPLC system consisting of LC-pump, PDA detector (λ=205 nm), autosampler (injection volume, 10 μL), and column oven (30 °C). The following parameters

were used for experiments: spray voltage, 5 kV; capillary temperature, 260 °C; and tube lens, 65 V. Nitrogen was used as sheath gas (50 arbitrary units) and auxiliary gas (5 arbitrary units). MS/MS experiments were performed by collision-induced decay (CID, 35 eV) mode. Helium served as the collision gas. The separations were performed by using a Macherey-Nagel Nucleodur Gravity C18 column (50×2 mm, 1.8 μm particle size) with a H_2O (+0.1 % HCOOH) (A)/ acetonitrile (+0.1 % HCOOH) (B) gradient (flow rate, 300 μL min^{-1}). Samples were analyzed by using a gradient program as follows: 80 % A isocratic for 2 min, linear gradient to 90 % B over 12 min, after 100 % B isocratic for 3.5 min, the system returned to its initial condition (80 % A) within 0.5 min, and was equilibrated for 6 min. The quantitation of the compounds was achieved by extraction of accurate masses (max. deviation, 2 ppm) of their quasimolecular ions $[M+H]^+$. An internal standard was used for calibration, since matrix effects could significantly influence the results of the MS measurements. The calibration graph was linear from a concentration of 2 to 5,000 ng mL^{-1}. The quantitation was achieved by plotting the ratio of the analyte signal to the internal standard signal as a function of the analyte concentration of the standards.

Sample preparation for AP-MALDI imaging

The biosensor strain (*C. violaceum*) was inoculated onto a thin NA layer plated over glass slides. After 24 h incubation at 30 °C, a 2,5-dihydroxybenzoic acid (DHB) matrix layer was applied on the biosensor colony through a new sprayer (TransMIT GmbH, Giessen—a brand name not relayed yet) for detection of C6-HSL. DHB (7 mg mL^{-1} in 50 % acetone, 49.9 % H_2O, and 0.1 % formic acid) was sprayed with the parameters 15.0 μL min^{-1} matrix flow, 4.5 L min^{-1} nitrogen gas flow, and 100 rpm sample platform drive with 40 min spray duration time. The sample was then subsequently measured. Images of the biosensor were taken with an optical microscope (Leica Microsystems, Wetzlar, Germany).

For measurement of C8-HSL, C10-HSL, and 3-oxo-C10-HSL, α-cyano-4-hydroxycinnamic acid (HCCA; 7 mg mL^{-1} in 50 % acetonitrile, 49.8 % H_2O, and 0.2 % trifluoroacetic acid) was sprayed with the parameters 15.0 μL min^{-1} matrix flow, 3.5 L min^{-1} nitrogen gas flow, 100 rpm sample platform drive for 2×20 min spray duration time. The sample was then air-dried and subsequently measured. Images of the biosensor were taken with an optical microscope (Leica Microsystems).

AP-MALDI imaging high-resolution mass spectrometry

Imaging experiments were performed with a Q-Exactive mass spectrometer (Thermo Fisher Scientific GmbH, Bremen, Germany) coupled to an atmospheric pressure (AP) MALDI ion source imagine10 (TransMIT GmbH, Giessen, Germany) using the full-scan mode (positive mode) within the mass range of *m*/*z* 100–400 (*R*=70,000 at *m*/*z*=200) with the internal lock masses of 273.03936 $[2M\text{-}2H_2O+H]^+$ (DHB) and 379.09246 $[2M+H]^+$ (HCCA), respectively. Acceleration voltage was set at 4 kV. A pulsed nitrogen laser (λ, 337.1 nm) at a frequency of 60 Hz with pulse duration times of 500 ms was used for generating UV radiation. Laser attenuation was set at 20 °C. Scan resolution was set at 40 and 100 μm.

Mirion (v.2.1.4.411) (TransMIT GmbH) mass spectrometry imaging software was used to create images from the obtained data/pixels with mass information. False colors were attached to masses with the corresponding pixel.

Sample preparation for UV-MALDI imaging

The biosensor strain (*C. violaceum*) was inoculated onto a thin NA layer plated over glass slides supplemented with various endophyte CFS concentrations. After 24 h incubation at 30 °C, a matrix layer (HCCA) was applied on the biosensor (colony) through a sprayer ImagePrep (Bruker Corporation, Bremen, Germany). HCCA (7 mg mL^{-1} in 50 % acetonitrile, 49.8 % H_2O, and 0.2 % trifluoroacetic acid) was sprayed three times. Sample wetness, matrix thickness, and incubation time were set at 4 (medium) on a relative scale from 1 to 7. Spray duration time was approximately 40 min for each spray cycle. The sample was then queued for subsequent measurement. Images of the biosensor challenged by endophyte CFS were documented with an optical microscope (Leica Microsystems).

UV-MALDI imaging high-resolution mass spectrometry

Imaging experiments were performed with a LTQ Orbitrap XL mass spectrometer coupled to a MALDI ion source (both from Thermo Fisher Scientific GmbH) using the Full-Scan mode (positive mode) within the mass range of *m*/*z* 100–400 (*R*=60,000 at *m*/*z* 200) with the internal lock masses of 273.03936 $[2M\text{-}2H_2O+H]^+$ (DHB) and 379.09246 $[2M+H]^+$ (HCCA), respectively. A pulsed nitrogen laser (λ=337.1 nm) was used for generating UV radiation. The sample was rastered with one microscan per step at a laser energy adjusted at 20 μJ. The scan resolution was set at 100 μm.

ImageQuest (v.1.0.1) (Thermo Fisher Scientific) mass spectrometry imaging software was used to create images from the obtained data/pixels with mass information. False colors were attached to masses with the corresponding pixel.

Results

Identification and characterization of the endophytic bacterial isolates

A total of 13 endophytic bacterial isolates were isolated from the *C. sativa* L. plants sampled from Bedrocan BV Medicinal

Cannabis (Veendam, the Netherlands). The isolates were identified and characterized by molecular identification based on 16S ribosomal RNA (rRNA) analysis. The amplified sequences spanning around 1,500 bp were used for the identification of the bacterial isolates. The PCR-amplified sequences were matched against the nucleotide database of the US National Centre for Biotechnology Information (NCBI) using the Basic Local Alignment Search Tool (BLASTn) for the identification of the bacterial isolates. The sequences were aligned using the EMBOSS-Pairwise Sequence Alignment of the EMBL Nucleotide Database. The sequences of the endophytic bacterial isolates have been deposited at EMBL-Bank. The identities of the endophytes were considered conspecific only at a minimum threshold identity of ≥98 % with the exception of only one isolate with 97 % sequence similarity. The accessions numbers with sequence similarities are detailed in Table 1.

Spectrophotometric quantitation of quorum quenching behavior

C. violaceum is a Gram-negative biosensor strain known to produce violacein, a purple pigment, as a result of quorum sensing utilizing the CviI/CviR synthase-receptor signaling (McClean et al. 1997). Loss of this pigment is indicative of quorum quenching behavior. For the preliminary selection of endophytic bacterial strains capable of quorum quenching, spectrophotometric quantitation of violacein was performed (Choo et al. 2006) using the CFS of the isolated endophytes. Four of the total isolated endophytic bacteria (*Bacillus* sp. strain B3, *Bacillus megaterium* strain B4, *Brevibacillus borstelensis* strain B8, and *Bacillus* sp. strain B11) exhibited significant potential in weakening the cell-to-cell quorum signals (C6-HSL, C8-HSL, C10-HSL, and 3-oxo-C10-HSL) of *C. violaceum* in a concentration-dependent manner (Fig. 1c–f). Furthermore, the CFU count assay confirmed that the CFS of isolates B3, B4, B8, and B11 did not impose any effect on the growth of *C. volaceum* but only reduced the violacein production (Fig. 1k). The logarithmic values of the bacterial count per milliliter (with replicates of each count) when treated with 8 mL CFS of each of the four bacterial isolates in comparison to control (untreated *C. violaceum*) is presented in Fig. 1k.

Quantification of quorum quenching behavior using HPLC-ESI-HRMS^n

The four strains (B3, B4, B8, and B11) were further analyzed in detail by LC-HRMS/MS using both external reference standards and an internal standard (d_3-C6-HSL) to quantify the exact amount of each of the AHLs being selectively quenched (Fig. 1a, b). In particular, the quorum sensing in *C. violaceum* was convened by all the four AHLs in different concentrations: the highest concentration was that of C10-HSL (2,088 ng/mL), followed by C8-HSL (320 ng/mL), 3-oxo-C10-HSL (7.1 ng/mL), and finally, C6-HSL (10.4 ng/mL) (Fig. 1g–j). Although C10-HSL was produced in higher concentration than C6-HSL signifying both CviR/C10-HSL- and CviR/C6-HSL-mediated regulation of signaling in this particular strain of *C. violaceum*, selective quorum quenching by the bacterial endophytes (Fig. 1g–j) corroborated earlier observations that C6-HSL is the primary and limiting autoinducer in *C. violaceum* (McClean et al. 1997). For example, the endophyte strain B11 quenched all the AHLs produced by the biosensor except C10-HSL (Fig. 1g–j). Interestingly, C6-HSL was quenched to less than half the concentration produced in the biosensor strain under control conditions (Fig. 1g) and concomitantly, there was a striking increase in the production of C10-HSL by the biosensor when challenged by endophyte strain B11. The same trend was also observed for strains B3, B4, and B8 (Fig. 1g–j).

Fig. 1 Quorum quenching of AHLs produced by biosensor strain *C. violaceum* by potent bacterial endophytes of *C. sativa* L. plants. **a** Representative LC-FTMS extracted ion chromatograms of detected AHLs (of control) quenched by CFS of endophytic bacterial strains (shown for strain B4). The ions monitored are displayed in each trace and correspond to the most abundant protonated molecules $[M+H]^+$ using a maximum deviation of 2 ppm. **b** Representative MS/MS spectra showing comparison of the main detected component, C10-HSL (*m/z* 256.1) in authenticated standard (*top*) and in the control biosensor strain (*bottom*). **c–f** Quorum quenching responses of the CFS of four endophytic bacterial strains (B3, B4, B8, and B11) against the biosensor strain *C. violaceum* (control). **g–j** Concentration of the different AHLs (ng mL^{-1}) quenched by the CFS extracts of the four endophytic bacterial strains B3, B4, B8, and B11. Control represents the biosensor strain *C. violaceum*. **k** Comparison of bacterial cell count of *C. violaceum* when treated with CFS extracts and when untreated (control). All the data represent the logarithmic value of CFU/mL (±SD)

Visualization of spatial distribution of quorum sensing signals and their quenching by endophytes using MALDI-imaging-HRMS

Since the production and release of AHLs range from intercellular to intracellular or extracellular, we investigated the spatial localization and distribution of the four AHLs in *C. violaceum* colony and periphery, and their quenching by endophytes using MALDI-Q-Exactive and MALDI-LTQ Orbitrap XL instruments. The resulting signal intensity was made visible by a color-coding system (Fig. 2) ranging from dark red (low intensity) to bright red (high intensity). Mass window was deliberately kept very small at Δ≤2 ppm from the theoretical masses for all the four AHLs measured. The untreated (not challenged by endophytes) *C. violaceum* showed visible production of violacein under the microscope (Fig. 2a, d), which was further sprayed with suitable matrix and shot by controlled laser beam. C6-HSL was produced by *C. violaceum* colony and released into the agar (Fig. 2c). The other three AHLs, namely C8-HSL (Fig. 2f), C10-HSL (Fig. 2g), and 3-oxo-C10-HSL (Fig. 2h) were not distributed far from the producing cells and only

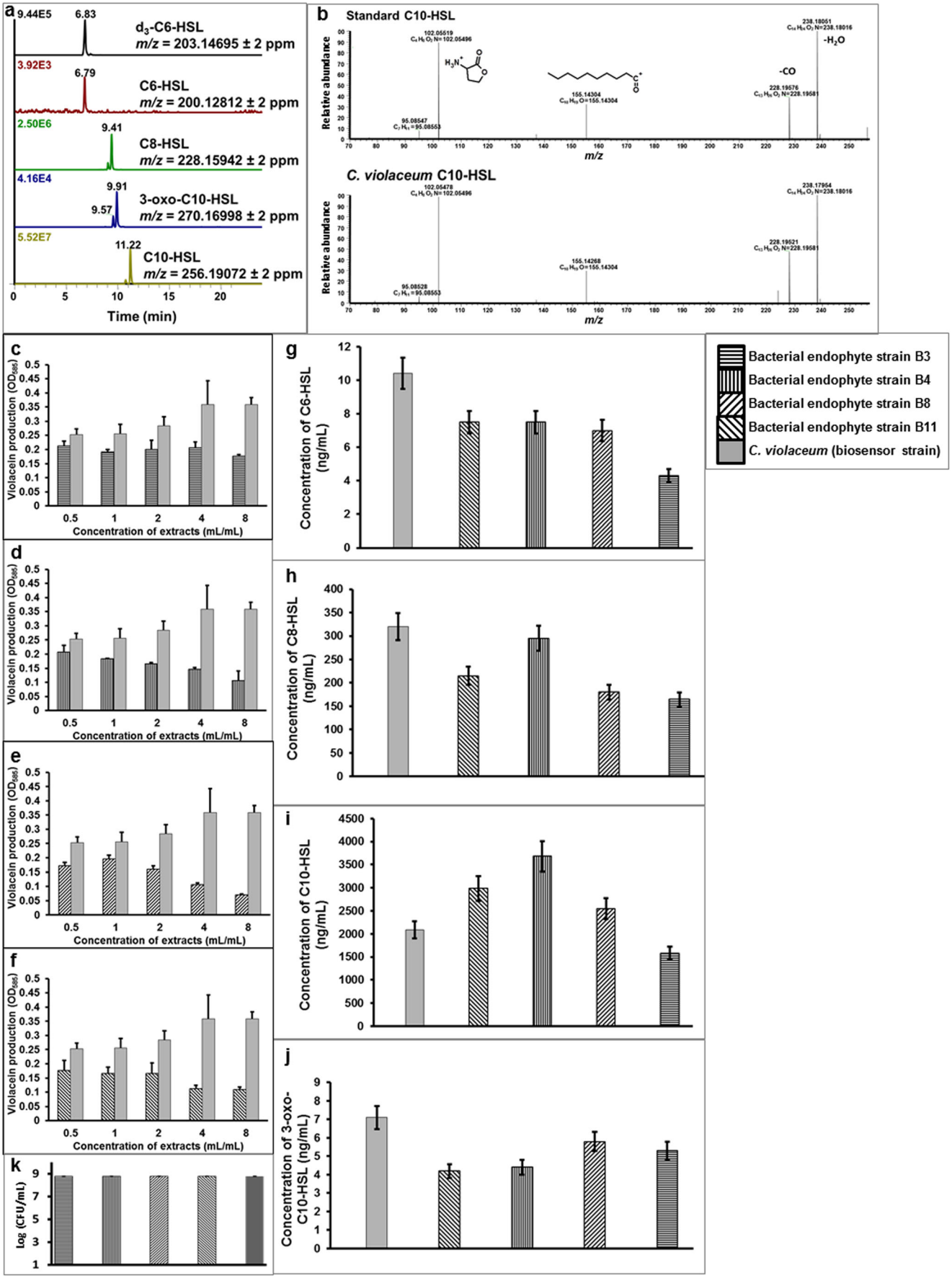
a
9.44E5
6.83
d3-C6-HSL
m/z = 203.14695 ± 2 ppm
3.92E3
6.79
C6-HSL
m/z = 200.12812 ± 2 ppm
2.50E6
9.41
C8-HSL
m/z = 228.15942 ± 2 ppm
4.16E4
9.91
9.57
3-oxo-C10-HSL
m/z = 270.16998 ± 2 ppm
5.52E7
11.22
C10-HSL
m/z = 256.19072 ± 2 ppm
Time (min)
b
Standard C10-HSL
-H2O
-CO
Relative abundance
m/z
C. violaceum C10-HSL
c
d
e
f
Violacein production (OD585)
Concentration of extracts (mL/mL)
g
Concentration of C6-HSL (ng/mL)
h
Concentration of C8-HSL (ng/mL)
i
Concentration of C10-HSL (ng/mL)
j
Concentration of 3-oxo-C10-HSL (ng/mL)
k
log (CFU/mL)
Bacterial endophyte strain B3
Bacterial endophyte strain B4
Bacterial endophyte strain B8
Bacterial endophyte strain B11
C. violaceum (biosensor strain)

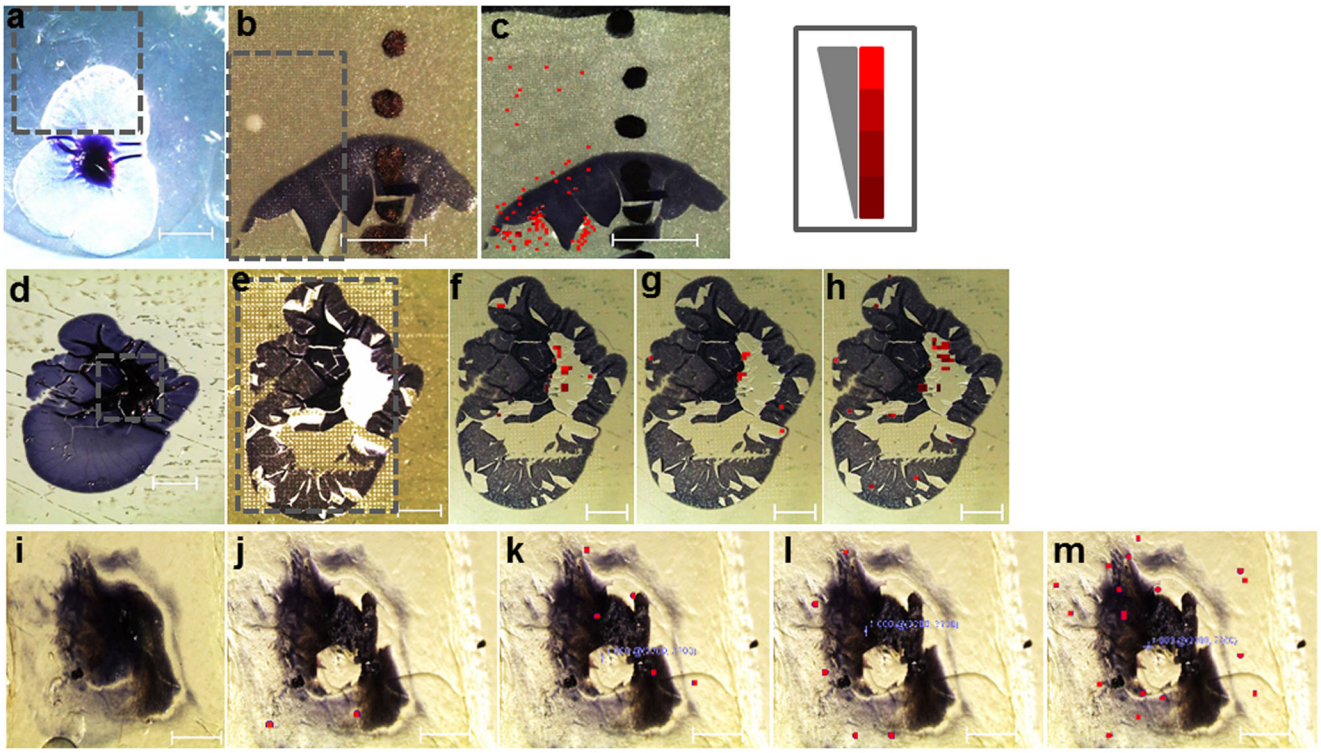

Fig. 2 Localization of the four different AHLs in the biosensor strain and their selective quenching by CFS extracts of the four endophytic bacterial strains B3, B4, B8, and B11. **a**, **d** Microscopic images of untreated (not challenged by endophyte CFS) *C. violaceum* showing visible production of violacein (violet color). *Gray-dotted insert* shows area explained in the text. **b**, **e** Microscopic images of *C. violaceum* after spraying with suitable matrix showing the crystals of uniform matrix covering the colony and its periphery. *Gray-dotted inserts* show areas shot by laser beam. **c** Localization of C6-HSL ($[M+H]^+$; m/z=200.12810; Δ<2 ppm). **f** Localization of C8-HSL ($[M+H]^+$; m/z=228.15940; Δ<2 ppm). **g** Localization of C10-HSL ($[M+H]^+$; m/z=256.19070; Δ<2 ppm). **h** Localization of 3-oxo-C10-HSL ($[M+H]^+$; m/z=270.16998; Δ<2 ppm). **i** Microscopic image of *C. violaceum* treated with CFS extract of bacterial endophyte strain B8. No visible production of violacein. **j** Remnants of C6-HSL after being quenched by CFS extract of bacterial endophyte strain B8 ($[M+H]^+$; m/z=200.12810; Δ<2 ppm). **k** Remnants of C8-HSL after being quenched by CFS extract of bacterial endophyte strain B8 ($[M+H]^+$; m/z=228.15940; Δ<2 ppm). **i** Remnants of C10-HSL after being quenched by CFS extract of bacterial endophyte strain B8 ($[M+H]^+$; m/z=256.19070; Δ<2 ppm). **m** Remnants of 3-oxo-C10-HSL after being quenched by CFS extract of bacterial endophyte strain B8 ($[M+H]^+$; m/z=270.16998; Δ<2 ppm). All *scale bars* represent 1 mm. *Insert gray box* shows the color-coded relative intensities of the detected AHLs in **c**, **f**–**h**, and **j**–**m**

accumulated in the nearest vicinity. In fact, these three AHLs accumulated directly below the colony (visualized after scraping off a part of the colony; see Fig. 2d gray dotted box). When *C. violaceum* was grown in agar containing the extracts of bacterial endophytes B4, B8, B11 and B3 at similar concentrations as that used in the violacein assay (see Fig. 1) for each AHL, selective quorum quenching was observed (Fig. 2j–m). The C6-HSL released profusely into the agar by *C. violaceum* was quenched by CFS of the endophytic bacterial isolates and only the remnants after being quenched were observed (Fig. 2j). Interestingly, C10-HSL and 3-oxo-C10-HSL were not only selectively quenched but also observed in the agar in the vicinity of the *C. violaceum* colony after quenching.

Discussion

In this study, we used a combination of HPLC-ESI-HRMS^n and matrix-assisted laser desorption ionization imaging high-resolution mass spectrometry (MALDI-imaging-HRMS) to quantify and visualize the spatial distribution of cell-to-cell quorum sensing signals in the biosensor strain, *C. violaceum*. We further investigated the quenching of the quorum sensing signals by potent endophytic bacterial isolates of medicinally important *C. sativa* plants. Our preliminary analysis of violacein production by *C. violaceum* and further quenching by selected bacterial isolates prompted us to study the specific modulation of the different AHLs convening quorum sensing in *C. violaceum*. A lot of research in the recent past has focused on different aspects of targeting the AHL signaling cascades for cell-to-cell communication in various microbial systems (Galloway et al. 2011; O'Loughlin et al. 2013). The implementation of MALDI-MS techniques has also gained importance in various aspects of research on microbial crosstalk. Recent studies have highlighted the use of such techniques in identification of microorganisms, clinical microbiology, and natural product biochemistry (Shih et al. 2014).

The four endophytic isolates showing potent quenching capability in the violacein assay were further analyzed using LC-HRMS/MS using both external reference standards and an internal standard. This provided a comprehensive understanding of the correlation between the endophytic bacterial species and their species-specific and selective ability of modulating different AHLs at different concentrations leading to an overall intervention of *C. violaceum* signaling cascade. Interestingly, we observed a trend of decreasing concentration of C6-HSL with an increase in the production of C10-HSL when treated with the CFS of endophytic bacterial isolates. This exemplified the fact that in *C. violaceum*, C10-HSL-mediated violacein production and transcription of *vio*A is inhibited by C6-HSL, as suggested by Morohoshi et al. (2010). It is further conceivable that *C. violaceum* triggered an increased production of C10-HSL as a counterstrategy when all other AHLs were being disrupted. Our work, thus, demonstrated that a single bacterial species can mount a multifaceted antivirulence defense strategy by simultaneously targeting the aggregation of different AHLs and modulate them at different concentration levels with the overall goal of minimizing the signaling potential of an invading pathogen. Studies on antiquorum activities within the scope of research on medicinal plants, using bioactive extracts from different sources against several pathogenic biosensor strains, are also gaining impetus (Kim and Park 2013; Lau et al. 2013; Samoilova et al. 2014). Such studies on different facets of microbial metabolism and crosstalk can serve an important tool for future biotechnological purposes (Safari et al. 2014).

Our investigation of the spatial localization and distribution of the four AHLs in *C. violaceum* by MALDI-imaging-HRMS revealed the release of C6-HSL on the periphery of the colony and successively diffusing into the agar. This finding corroborated the concept of CviI/CviR synthase receptor-regulated C6-HSL production followed by free passive diffusion across the cell envelope to accumulate in the local environment (McClean et al. 1997; LaSarre and Federle 2013). This visually confirmed in high spatial resolution that in *C. violaceum*, C6-HSL is first released into the extracellular environment after production which might then be taken up by another cell in the same population to begin violacein production (McClean et al. 1997). The other three AHLs (C8-HSL, C10-HSL, and 3-oxo-C10-HSL) did not diffuse freely into the agar and were found accumulating in the immediate vicinity of *C. violaceum* that could only be visualized directly below the colony itself. These AHLs were not passively released into the agar as compared to C6-HSL, revealing that they might be actively transported across the cell membrane in a controlled manner as suggested by LaSarre and Federle (2013). The biosensor strain, when treated with the CFS of endophytic bacterial isolates, displayed selective quorum quenching of all the four AHLs. This visually confirmed the differential quorum quenching abilities of the selected bacterial endophytes. Interestingly, C10-HSL and 3-oxo-C10-HSL remnants were observed in the agar in the vicinity of the *C. violaceum* colony, lending evidence to the fact that the endophytes were capable not only of preventing the production of these AHLs by the biosensor strain but also possibly stalled their active transportation post-production.

This study provides fundamental insights into the potential of endophytic bacteria as biocontrol agents against bacterial phytopathogens as well as antivirulence agents that might be useful in quorum-inhibiting therapies. Almost all Gram-negative bacterial pathogens maintain pathogenicity in their hosts (plants or animals, including humans) by cell-to-cell communication using quorum sensing signaling (Sifri 2008; Morohoshi et al. 2013; Amaral et al. 2014; Christiaen et al. 2014; Schafhauser et al. 2014). Attenuation of these signals will lead to suppression of pathogen virulence without introducing additional resistance-inducing selection pressures. It is well-known that endophytes are capable of maintaining mutualistic associations with their host plants over a period of their life cycle (Kusari et al. 2012, 2013, 2014), which might lead to co-evolution of certain functional traits (such as production of bioactive secondary metabolites). However, during their co-existence with host plants, endophytes encounter invasion by a plethora of specific and generalist pathogens. Therefore, in order to survive in their ecological niches (internal plant environment), endophytes might evolve additional defense strategies that prevent the pathogens from developing resistance to their arsenal of bioactive secondary metabolites (used in chemical defense). Quorum quenching is one of such antivirulence strategies that are developed by selected endophytic bacteria. This work, thus, highlights an important biological role played by endophytes in different ecological niches, not only in host plant defense but also in maintaining colonization and their own survival inside plants. Interestingly, the bacterial interactions and antivirulence strategies might differ in environmental niches where different microbial communities interfere with the signaling systems. Recently for example, challenges of multiple signaling in bacterial communities in a particular environment with regard to their perception of different signaling molecules, have been highlighted (Cornforth et al. 2014). Admittedly, our work provides the insights into quorum quenching strategies employed by endophytic bacteria against a single biosensor strain. These quenching strategies might differ during multiple signaling events under different environmental conditions. Our study, however, provides a scientific handle to further investigate in planta quorum quenching by endophytes and elucidate the exact role of AHL-mediated gene expression and regulation within complex ecological niches of multi-species microbial communities.

Acknowledgments This research was funded by the Ministry of Innovation, Science and Research of the German Federal State North Rhine-Westphalia (NRW) and TU Dortmund by a scholarship to P.K. from the CLIB-Graduate Cluster Industrial Biotechnology. We thank the German Research Foundation (DFG) for financing the MALDI imaging high-resolution mass spectrometers. We are thankful to Federal Institute for Drugs and Medical Devices (Bundesinstituts für Arzneimittel und Medizinprodukte, BfArM), Bonn, Germany for granting us the necessary permissions for working with *Cannabis* plants (BtM number 458 49 89). S.K. was a Visiting Researcher at the Department of Plant Sciences, University of Oxford, South Parks Road, Oxford OX1 15 3RB, UK, during part of the work and preparation of the manuscript (Apr 2013 to Mar 2014). S.K. gratefully acknowledges M.S. for approving and authorizing, Dr. Gail M. Preston for hosting, and TU Dortmund for supporting his stay at the University of Oxford.

Conflict of Interest The authors declare no conflict of interest.

References

Aly AH, Debbab A, Proksch P (2013) Fungal endophytes—secret producers of bioactive plant metabolites. Pharmazie 68:499–505

Amara N, Krom BP, Kaufmann GF, Meijiler MM (2011) Macromolecular inhibition of quorum sensing: enzymes, antibodies, and beyond. Chem Rev 111:195–208

Amaral L, Martins A, Spengler G, Molnar J (2014) Efflux pumps of Gram-negative bacteria: what they do, how they do it, with what and how to deal with them. Front Pharmacol 4:168. doi:10.3389/fphar.2013.00168

Bjarnholt N, Li B, D'Alvise J, Janfelt C (2014) Mass spectrometry imaging of plant metabolites—principles and possibilities. Nat Prod Rep. doi:10.1039/c3np70100j

Burmølle M, Thomsen TR, Fazli M, Dige I, Christensen L, Homøe P, Tvede M, Nyvad B, Tolker-Nielsen T, Givskov M, Moser C, Kirketerp-Møller K, Johansen HK, Høiby N, Jensen P, Sørensen SJ, Bjarnsholt T (2010) Biofilms in chronic infections—a matter of opportunity—monospecies biofilms in multispecies infections. FEMS Immmunol Med Microbiol 59:324–336

Choo JH, Rukayadi Y, Hwang J-K (2006) Inhibition of bacterial quorum sensing by vanilla extract. Lett Appl Microbiol 42:637–641

Christiaen SEA, Matthijs N, Zhang X-H, Nelis HJ, Bossier P, Coenye T (2014) Bacteria that inhibit quorum sensing decrease biofilm formation and virulence in *Pseudomonas aeruginosa* PAO1. Pathog Dis 70:271–279

Claessen D, Rozen DE, Kuipers OP, Søgaard-Andersen L, van Wezel GP (2014) Bacterial solutions to multicellularity: a tale of biofilms, filaments and fruiting bodies. Nat Rev Microbiol. doi:10.1038/nrmicro3178

Clatworthy AE, Pierson E, Hung DT (2007) Targeting virulence: a new paradigm for antimicrobial therapy. Nat Chem Biol 3:541–548

Cornforth DM, Popat R, McNally L, Gurney J, Scott-Phillips TC, Ivens A, Diggle SP, Brown SP (2014) Combinatorial quorum sensing allows bacteria to resolve their social and physical environment. Proc Natl Acad Sci U S A 111:4280–4284

Galloway WRJD, Hodgkinson JT, Bowden SD, Welch M, Spring DR (2011) Quorum sensing in Gram-negative bacteria: small-molecule modulation of AHL and AI-2 quorum sensing pathways. Chem Rev 111:28–67

Grotenhermen F, Müller-Vahl K (2012) The therapeutic potential of *Cannabis* and cannabinoids. Dtsch Arztebl Int 109:495–501

Hosni T, Moretti C, Devescovi G, Suarez-Moreno ZR, Fatmi MB, Guarnaccia C, Pongor S, Onofri A, Buonaurio R, Venturi V (2011) Sharing of quorum-sensing signals and role of interspecies communities in a bacterial plant disease. ISME J 5:1857–1870

Kharwar RN, Mishra A, Gond SK, Stierle A, Stierle D (2011) Anticancer compounds derived from fungal endophytes: their importance and future challenges. Nat Prod Rep 28:1208–1228

Kim S-H, Park H-D (2013) Ginger extract inhibits biofilm formation by *Pseudomonas aeruginosa* PA14. PLoS ONE 8:e76106

Kusari S, Spiteller M (2011) Are we ready for industrial production of bioactive plant secondary metabolites utilizing endophytes? Nat Prod Rep 28:1203–1207

Kusari S, Zühlke S, Spiteller M (2009a) An endophytic fungus from *Camptotheca acuminata* that produces camptothecin and analogues. J Nat Prod 72:2–7

Kusari S, Lamshöft M, Spiteller M (2009b) *Aspergillus fumigatus* Fresenius, an endophytic fungus from *Juniperus communis* L. Horstmann as a novel source of the anticancer pro-drug deoxypodophyllotoxin. J Appl Microbiol 107:1019–1030

Kusari S, Hertweck C, Spiteller M (2012) Chemical ecology of endophytic fungi: origins of secondary metabolites. Chem Biol 19:792–798

Kusari P, Kusari S, Spiteller M, Kayser O (2013) Endophytic fungi harbored in *Cannabis sativa* L.: diversity and potential as biocontrol agents against host plant-specific phytopathogens. Fungal Divers 60:137–151

Kusari S, Singh S, Jayabaskaran C (2014) Biotechnological potential of plant-associated endophytic fungi: hope versus hype. Trends Biotechnol. doi:10.1016/j.tibtech.2014.03.009

Lane DJ (1991) 16S/23S rRNA sequencing. In: Stackebrandt E, Goodfellow M (eds) Nucleic acid techniques in bacterial systematics. Wiley, New York, pp 115–175

LaSarre B, Federle MJ (2013) Exploiting quorum sensing to confuse bacterial pathogens. Microbiol Mol Biol Rev 77:73–111

Lau YY, Sulaiman J, Chen JW, Yin W-F, Chan K-G (2013) Quorum sensing activity of *Enterobacter asburiae* isolated from lettuce leaves. Sensors 13:14189–14199

Limsuwan S, Voravuthikunchai SP (2008) *Boesenbergia pandurata* (Roxb.) Schltr., *Eleutherine americana* Merr. and *Rhodomyrtus tomentosa* (Aiton) Hassk. as antibiofilm producing and antiquorum sensing in *Streptococcus pyogenes*. FEMS Immunol Med Microbiol 53:429–436

Márquez LM, Redman RS, Rodriguez RJ, Roossinck MJ (2007) A virus in a fungus in a plant: three way symbiosis required for thermal tolerance. Science 315:513–515

McClean KH, Winson MK, Fish L, Taylor A, Chhabra SR, Camara M, Daykin M, Lamb JH, Swift S, Bycroft BW, Stewart GSAB, Williams P (1997) Quorum sensing and *Chromobacterium violeceum*: exploitation of violacein production and inhibition for the detection of *N*-acyl homoserine lactones. Microbiology 143:3703–3711

Morohoshi T, Fukamachi K, Kato M, Kato N, Ikeda T (2010) Regulation of the violacein biosynthetic gene cluster by acylhomoserine lactone-mediated quorum sensing in *Chromobacterium violaceum* ATCC 12472. Biosci Biotechnol Biochem 74:2116–2119

Morohoshi T, Tokita K, Ito S, Saito Y, Maeda S, Kato N, Ikeda T (2013) Inhibition of quorum sensing in gram-negative bacteria by alkylamine-modified cyclodextrins. J Biosci Bioeng 116:175–179

O'Loughlin CT, Miller LC, Siryaporn A, Drescher K, Semmelhack MF, Bassler BL (2013) A quorum-sensing inhibitor blocks *Pseudomonas aeruginosa* virulence and biofilm formation. Proc Natl Acad Sci U S A 110:17981–17986

Ou CC, Lu TM, Tsai JJ, Yen JH, Chen HW, Lin MY (2009) Antioxidative effect of lactic acid bacteria: intact cells vs. intracellular extracts. J Food Drug Anal 17:209–216

Porras-Alfaro A, Bayman P (2011) Hidden fungi, emergent properties: endophytes and microbiomes. Annu Rev Phytopathol 49:291–315

Rasko DA, Sperandio V (2010) Anti-virulence strategies to combat bacteria-mediated disease. Nat Rev Drug Discov 9:117–128

Rishi P, Preet S, Kaur P (2011) Effect of *L. plantarum* cell-free extract and co-trimoxazole against *Salmonella typhimurium*: a possible adjunct therapy. Ann Clin Microbiol Antimicrob 10:9

Rompp A, Spengler B (2013) Mass spectrometry imaging with high resolution in mass and space. Histochem Cell Biol 139:759–783

Safari M, Amache R, Esmaeilishirazifard E, Keshavarz T (2014) Microbial metabolism of quorum-sensing molecules acyl-homoserine lactones, γ-heptalactone and other lactones. Appl Microbiol Biotechnol 98: 3401–3412

Samoilova Z, Muzyka N, Lepekhina E, Oktyabrsky O, Smirnova G (2014) Medicinal plant extracts can variously modify biofilm formation in *Escherichia coli*. A Van Leeuw J Microb 105:709–722

Schafhauser J, Lepine F, McKay G, Ahlgren HG, Khakimova M, Nguyen D (2014) The stringent response modulates 4-hydroxy-2-alkylquinoline biosynthesis and quorum-sensing hierarchy in *Pseudomonas aeruginosa*. J Bacteriol 196:1641–1650

Schulz B, Guske S, Dammann U, Boyle C (1998) Endophyte-host interactions II. Defining symbiosis of the endophyte-host interaction. Symbiosis 25:213–227

Shih C-J, Chen P-Y, Liaw C-C, Lai Y-M, Yang Y-L (2014) Bringing microbial interactions to light using imaging mass spectrometry. Nat Prod Rep. doi:10.1039/c3np70091g

Sifri CD (2008) Quorum sensing: bacteria talk sense. Clin Infect Dis 47: 1070–1076

Taura F, Sirikantaramas S, Shoyamaa Y, Shoyamaa Y, Morimotoa S (2007) Phytocannabinoids in *Cannabis sativa*: recent studies on biosynthetic enzymes. Chem Biodivers 4:1649–1663

Teplitski M, Mathesius U, Rumbaugh KP (2011) Perception and degradation of *N*-acyl homoserine lactone quorum sensing signals by mammalian and plant cells. Chem Rev 111:100–116

Thenmozhi R, Nithyanand P, Rathna J, Pandian SK (2009) Antibiofillm activity of coral-associated bacteria against different clinical M serotypes of *Streptococcus pyogenes*. FEMS Immunol Med Microbiol 57:284–294

Zhao Q, Mutukumira A, Lee SJ, Maddox I, Shu Q (2011) Functional properties of free and encapsulated *Lactobacillus reuteri* DPC16 during and after passage through a simulated gastrointestinal tract. World J Microbiol Biotechnol 28:61–70